

Spatial variation of the magnetic field inside laminar flows of a perfect conductive fluid

This content has been downloaded from IOPscience. Please scroll down to see the full text.

2017 Eur. J. Phys. 38 015806

(<http://iopscience.iop.org/0143-0807/38/1/015806>)

View [the table of contents for this issue](#), or go to the [journal homepage](#) for more

Download details:

IP Address: 61.129.42.30

This content was downloaded on 13/12/2016 at 16:56

Please note that [terms and conditions apply](#).

Spatial variation of the magnetic field inside laminar flows of a perfect conductive fluid

Bejo Duka¹ and Sonila Boçi

Department of Physics, Faculty of Natural Sciences, University of Tirana, Tirana, Albania

E-mail: bejo.duka@unitir.edu.al and sonila.boci@fshn.edu.al

Received 27 July 2016, revised 5 November 2016

Accepted for publication 11 November 2016

Published 13 December 2016



CrossMark

Abstract

The steady state of a perfect conductive fluid in laminar flow resulting from the ‘Hall effect’ is studied. Using the Maxwell equations, the spatial variation of the magnetic field in the steady state is calculated for three cases of different fluid flow geometries: flow between two infinite parallel planes, flow between two coaxial infinite-long cylinders and flow between two concentric spheres. According to our calculation of the three cases, the spatial variation of the magnetic field depends on the flow velocity. The magnetic field is strengthened in layers where the velocity is greater, but this dependency is negligible for non relativistic flows. Our approach in this study provides an example of how to receive interesting results using only basic knowledge of physics and mathematics.

Keywords: magnetic field, fluid flow, dynamo action, Hall effect

1. Introduction

Conductive fluid and plasma flows with magnetic field implications are subjects of great interest in physics, geophysics and astrophysics. Different kinds of flow are studied using different approaches. Some flows of a simplified configuration represent theoretical or didactic interest. Meanwhile flows of a quite complicated configuration are studied in order to gain insight into the mechanisms of magnetic field generation and sustainability in celestial bodies such as the Earth or stars.

Dynamo action is an instability mechanism by which part of the mechanical energy is converted into magnetic energy by the motion of an electrically conductive fluid (Moffatt 1978). As a conductive fluid flows across the magnetic field lines, an electrical current associated with a magnetic field is induced. When this magnetic field reinforces the original

¹ Author to whom any correspondence should be addressed.

magnetic field, a *dynamo action* is produced that can compensate for the magnetic field diffusion (Inglis 1981). Depending on the relationship between the flow and the magnetic field, the induced magnetic field can reinforce the pre-existing magnetic field; such a system is considered to be a self-sustaining dynamo. It is believed that this effect is at the origin of the magnetic fields of planets and most astrophysical objects (e.g. Parker 1979, Fearn 1998, Weiss 2002, Charbonneau 2014; etc). In these objects, dynamo action is conditioned by the presence of highly conductive fluids like the Earth's liquid iron in the outer core, or the ionized gas of the Sun. In contrast to the technical dynamo which relies through its wiring on a multiple connected distribution of electric conductivity, the homogeneous dynamo operating in planetary cores and in stars depends on a sufficiently complex structure of fluid and plasma motions.

Dynamo theory uses magnetohydrodynamic (MHD) equations to investigate how the flow of the conductive materials of astrophysical bodies can continuously regenerate these magnetic fields (e.g. Roberts and Soward 1992, Jones 2011). Large scale computations are necessary to solve numerically MHD equations of dynamo theory, i.e. to simulate the dynamo process (e.g. Kuang and Bloxham 1997, Sarson and Jones 1999, Roberts and Glatzmaier 2000). The dynamo simulations represent rough approximations of the processes occurring in the Earth's core, and the results are often so complicated that they are difficult to understand (Love 1999).

Since the first tentative experiments on the kinematic dynamo effect (Lowes and Wilkinson 1963), now there are several successful experimental setups of fluid or plasma flow in similar conditions as in the Earth's outer core (e.g. Stieglitz and Muller 2001, Gailitis *et al* 2002, Marie *et al* 2002, Müller and Stieglitz 2002, Monchaux *et al* 2007, Spence *et al* 2009, Giesecke *et al* 2012, Cooper *et al* 2014) where different aspects of the dynamo processes are studied.

In the present work, some idealized fluid flows, when a uniform magnetic field is applied on them, are studied. We aimed to investigate if such flows could present any kind of dynamo action and what the magnetic field reconfiguration in the steady state of such flows would look like. Starting from some kind of 'Hall effect' and using classical methods of electrodynamics, the spatial reconfiguration of the magnetic field in the fluid flow is calculated. The known 'Hall effect' results from an asymmetry of charge distribution in a conductive medium when a magnetic field perpendicular to the motion of charges is applied. This effect can be measured experimentally as the 'Hall voltage' difference between the extremes of this charge separation (e.g. Kunkel 1981, Petersen *et al* 2008).

The laminar flows of perfect conductive fluids are considered here. The infinite conductivity approximation could be reasonable for the Earth's outer core liquid (where the upper bound of the conductivity is evaluated to be 10^6 S m^{-1}) or for solar gas (where the conductivity, which depends on temperature, is high except photosphere and lower chromosphere (Stix 2002)). The considered laminar flows are confined between: (a) two infinite planes, (b) two infinite long cylinders and (c) two concentric spheres. When an initial uniform magnetic field is applied to these flows, instant currents are induced. These currents terminate to a redistribution of the charges flowing in a steady state and so producing the new magnetic field configuration. According to our calculations, the spatial variation of this field presents a 'strengthening' effect in the sense that the ratio of the magnetic field values (B_2/B_1) in two different layers is greater than 1 when the velocities in these layers are $v_1 < v_2$.

The studied cases can be used as complex exercises in an intermediary course on 'classical electrodynamics' or in an introductory course on MHD for undergraduate students.

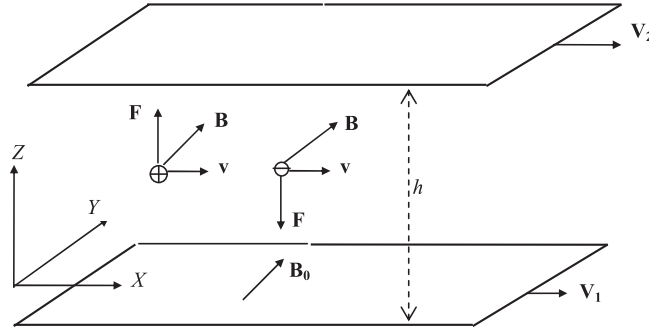


Figure 1. Lorentz forces on the positive and negative charges are in the opposite directions.

2. Magnetic field reconfiguration due to the Hall effect

When a magnetic field \mathbf{B} is applied to an electric current flow of density $\mathbf{J} = nq\mathbf{v}$, where q is the charge and n is the number density of the free charges moving with velocity \mathbf{v} , due to the Lorentz force ($\mathbf{F} = q\mathbf{v} \times \mathbf{B}$), the charges drift perpendicularly to the current flow direction and to the magnetic field. In the steady state, there is a redistribution of the charges which produces the electric field: $\mathbf{E} = -\mathbf{v} \times \mathbf{B}$ inside the conductor that holds back further charge drift.

The balance of forces can be written in the form (Moelter *et al* 1998)

$$\mathbf{E} + \frac{1}{nq}\mathbf{J} \times \mathbf{B} = \frac{1}{\sigma}\mathbf{J} \quad (1)$$

where σ is the specific conductivity. Imaging that any resistivity on the direct movement of charges is absent² i.e. considering a perfect electrical conductivity ($\sigma = \infty$), we have

$$\mathbf{E} + \frac{1}{nq}\mathbf{J} \times \mathbf{B} = \mathbf{E} + \mathbf{v} \times \mathbf{B} = 0. \quad (2)$$

In the context of an ‘ideal MHD approximation’, (2) can be regarded as the limit of a constitutive relation such as Ohm’s law (see equation 3.8 in Ogilvie (2016)).

In most conductors, such as metals, the Hall effect is very small because the density of conduction electrons is large (the order of 10^{29} m^{-3}). While in semiconductors and many plasmas n is several orders of magnitude smaller. Therefore, the effect is much more pronounced in both semiconductors and low-density plasmas which have comparatively low densities of charge carriers (Kunkel 1981).

2.1. Planar geometry

We assume that a perfect electrically conductive fluid fills the space between two solid planes (isolator plates) that are parallel to the XY plane with the distance $h = \text{constant}$ between them (figure 1). The solid infinite planes move in the X direction with different velocities producing a laminar fluid flow in this direction. This flow is not a uniform one, it has different values of

² Charge carrier collisions of their chaotic movement that provide resistivity to the direct movement are neglected, therefore the resistivity is zero and its reversal (the conductivity) is infinity.

velocities at different altitudes z [$v = v_x = v(z)$], from V_1 in the lower plane to V_2 in the upper plane.

The fluid flow is considered electrically neutral: the same numbers of positive ($+q$) and negative ($-q$) ions are uniformly distributed in the fluid. Let \mathbf{B}_0 be an initial uniform magnetic field applied in the Y -axis direction, created by the sources outside the planes.

Due to the Lorentz force (see figure 1), the differentiation of electric charge concentration ($\rho(z)$) occurs, the positive charges are moved upward and the negative ones are moved downward. Such charge differentiation creates an electrical field \mathbf{E} inside the fluid that opposes the further charge differentiation. In the steady state, the Lorentz force is balanced by the electrical force. As the differentiated charges, being in the different layers, move with different velocities, then a net electric current in the X direction arises. The magnetic field of such a current has the same direction as the initial external field \mathbf{B}_0 .

In the steady state we have

$$q\mathbf{E} = -q\mathbf{v} \times \mathbf{B} \quad \Rightarrow \quad E = E_z = -v_x B_y = -v B. \quad (3)$$

The Maxwell equations can be written (Jackson 1999)

$$\nabla \times \mathbf{B} = \mu_0 \rho \mathbf{v} \quad \Rightarrow \quad -\frac{dB}{dz} = \mu_0 \rho v \quad (4)$$

$$\nabla \cdot \mathbf{E} = \frac{\rho}{\varepsilon_0} \quad \Rightarrow \quad \frac{dE}{dz} = \frac{\rho}{\varepsilon_0}, \quad (5)$$

where ρ is the volume density of charges. From equation (3), one can see that when the fluid is at rest ($v = 0$, when $V_1 = V_2 = 0$) the electric field vanishes everywhere in the fluid, therefore its divergence goes to zero ($\nabla \cdot \mathbf{E} \rightarrow 0$) and from equation (5), one can see that $\rho \rightarrow 0$; i.e. the positive and negative charges have the same density, balancing each other, and the fluid is electro-neutral everywhere.

From (3)–(5), we find

$$\frac{dB}{dz} = \varepsilon_0 \mu_0 v \frac{d(vB)}{dz},$$

which can be transformed to

$$\frac{dB}{B} = -\frac{1}{2} \frac{d(1 - \varepsilon_0 \mu_0 v^2)}{(1 - \varepsilon_0 \mu_0 v^2)}. \quad (6)$$

Integration of equation (6) provides the spatial configuration of the magnetic field in the steady state

$$B(z) = B_1 \frac{\sqrt{1 - V_1^2/c^2}}{\sqrt{1 - v^2(z)/c^2}}, \quad (7)$$

where B_1 is the value of the magnetic field at the lower plate (not defined).

Integration of equation (6) in the boundaries of fluid layers: from z_1 (where the velocity is v_1 and the magnetic field B_1) to z_2 (where the velocity is v_2 and the field is B_2), provides

$$\frac{B_2}{B_1} = \frac{\sqrt{1 - v_1^2/c^2}}{\sqrt{1 - v_2^2/c^2}}, \quad (8)$$

where the constant $c = (1/\varepsilon_0 \mu_0)^{1/2}$ is the light velocity in vacuum ($300\,000 \text{ km s}^{-1}$). If $v_1 < v_2$ then $B_2 > B_1$, i.e. the magnetic field is strengthened in the Z direction. But this

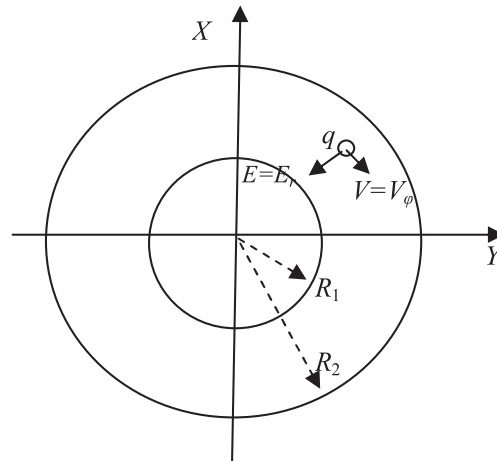


Figure 2. Induced electric field and positive charge velocity.

strengthening is negligible because for any fluid flow (non relativistic) the velocities are much smaller than the light velocity ($c \gg v_1$ and $c \gg v_2$). From (8), it is derived that

$$\frac{B_2}{B_1} \approx 1 + \frac{v_2^2 - v_1^2}{2c^2}; \text{ as } v_2^2 - v_1^2 \ll c^2 \text{ then } B_1 \approx B_2.$$

2.2. Cylindrical geometry

In this case the fluid flows between two coaxial solid insulator cylinders that rotate with the same angular velocity ω about the same axis of rotation (Z axis in the figure 2). The cylinders are extended to the infinity along Z -axis (cylindrical coordinates: r, φ, z). The fluid velocity is the simplest case of the flows between rotating cylinders given by Landau and Lifshitz (1987)

$$v = v_\varphi = \omega r, \quad (9)$$

with $V_1 = \omega R_1$ at the boundary of the inner cylinder and $V_2 = \omega R_2$ at the boundary of the outer cylinder.

Let be \mathbf{B}_0 an initial uniform magnetic field parallel to the Z -axis. By the symmetry regarding this axis, in the steady regime a radial differentiation of positive and negative charges is settled. The differentiated charges move with different velocities and a net electric current in the azimuthal direction (\mathbf{e}_φ) arises. The magnetic field of such a current has the same direction Z as the external field \mathbf{B}_0 .

In the steady state we have

$$q\mathbf{E} = -q\mathbf{v} \times \mathbf{B} \quad \Rightarrow \quad E = E_r = -v_\varphi B_z = -v B. \quad (10)$$

From the Maxwell equations (Jackson 1999), in the cylindrical coordinates, we obtain

$$\nabla \times \mathbf{B} = \mu_0 \rho \mathbf{v} \quad \Rightarrow \quad -\frac{dB}{dr} = \mu_0 \rho v \quad (11)$$

$$\nabla \cdot \mathbf{E} = \frac{\rho}{\varepsilon_0} \Rightarrow \frac{1}{r} \frac{d(rE_r)}{dr} = \frac{\rho}{\varepsilon_0}. \quad (12)$$

From (10)–(12), we find

$$\frac{1}{r} \frac{d}{dr}(rvB) = \frac{1}{\varepsilon_0 \mu_0 v} \frac{dB}{dr}. \quad (13)$$

Substituting here $v = \omega r$, we get

$$\frac{\omega}{c^2} \frac{d(r^2\omega)}{dr} = \frac{1}{B} \frac{dB}{dr} \quad (14)$$

$$1 - \frac{r^2\omega^2}{c^2}$$

or

$$-\frac{d\left(1 - \frac{r^2\omega^2}{c^2}\right)}{1 - \frac{r^2\omega^2}{c^2}} = \frac{dB}{B}. \quad (15)$$

Integration of equation (15) provides the spatial configuration of the magnetic field in the steady state

$$B = B_1 \frac{\left(1 - \frac{R_1^2\omega^2}{c^2}\right)}{\left(1 - \frac{r^2\omega^2}{c^2}\right)}. \quad (16)$$

The integration of equation (15) from $r = R_1$ to $r = R_2$, gives

$$\frac{B_2}{B_1} = \frac{\left(1 - \frac{R_1^2\omega^2}{c^2}\right)}{\left(1 - \frac{R_2^2\omega^2}{c^2}\right)}. \quad (17)$$

As $R_2 > R_1$, there is a magnetic field strengthening in the radial direction. But this strengthening is negligible for any non relativistic fluid flow.

It is noted that comparing the magnetic field ratio (17) in the case of cylindrical geometry with the same ratio in the case of the infinite planar geometry (8), the first ratio is more powerful (in power two of the ratio of the plane geometry case). This can be explained by the difference between the two cases: in the case of infinite planes there is an infinity extension in the two directions X, Y , while in the case of cylindrical geometry there is an infinity extension only in one direction (Z).

Cylindrical geometry is used in cases of experimental interest, for example: the hydro-magnetic fluid flow on a porous rotating disk in the presence of an axial uniform magnetic steady field with inclusion of Hall current effects is studied by obtaining an analytical solution (Turkyilmazoglu 2012) or using numerical solutions (Turkyilmazoglu 2010).

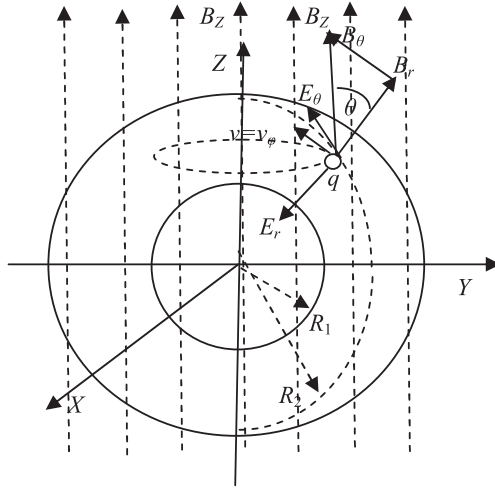


Figure 3. Induced electric field and initial magnetic field, and positive charge velocity.

2.3. Spherical geometry

We considered two solid concentric insulator spheres: the inner one with radius R_1 and outer one with radius R_2 , both rotating with a constant angular velocity ω around the Z -axis (figure 3). A perfect conductive fluid fills the gap between the inner and outer spherical solid boundaries. In the spherical coordinates r, θ, φ , the velocity field in the fluid can be found (e.g. Landau and Lifshitz 1987, Duka 1999)

$$v = v_\varphi = \omega r \sin \theta. \quad (18)$$

Suppose that initially there is a uniform magnetic field directed in the Z -direction

$$\mathbf{B} = B_z \cos \theta \cdot \mathbf{e}_r - B_z \sin \theta \cdot \mathbf{e}_\theta. \quad (19)$$

It acts in opposite directions on positive and negative electric charges of the fluid. In the steady state, there is an electric field created by the differentiation of charges, which has two components (E_r and E_θ)

$$\mathbf{E} = -\mathbf{v} \times \mathbf{B} = -B_z \omega r \sin^2 \theta \mathbf{e}_r - B_z \omega r \sin \theta \cos \theta \mathbf{e}_\theta, \quad (20)$$

while the curl of the magnetic field has only one component in the φ -direction

$$\nabla \times \mathbf{B} = \frac{1}{r} \left[\frac{\partial}{\partial r} (r B_\theta) - \frac{\partial B_r}{\partial \theta} \right] \mathbf{e}_\varphi = \frac{1}{r} \left[\frac{\partial}{\partial r} (-r \sin \theta B_z) - \frac{\partial (B_z \cos \theta)}{\partial \theta} \right] \mathbf{e}_\varphi. \quad (21)$$

According to the Maxwell equations, this curl is

$$\nabla \times \mathbf{B} = \mu_0 \rho \mathbf{v} \quad (22)$$

where the charge density can be substituted by the equation

$$\rho = \varepsilon_0 \nabla \cdot \mathbf{E} = \varepsilon_0 \left[\frac{1}{r^2} \frac{\partial}{\partial r} (-B_z \omega r^3 \sin^2 \theta) + \frac{1}{r \sin \theta} \frac{\partial}{\partial \theta} (-B_z \omega r \sin^2 \theta \cos \theta) \right]. \quad (23)$$

Substituting (23) and (21) in (22) and $\varepsilon_0 \mu_0 = 1/c^2$, we find

$$\frac{\sin \theta}{r} \frac{\partial}{\partial r}(rB_z) + \frac{1}{r} \frac{\partial}{\partial \theta}(B_z \cos \theta) = \frac{\omega^2 \sin^3 \theta}{c^2 r} \frac{\partial}{\partial r}(r^3 B_z) + \frac{\omega^2 r}{c^2} \frac{\partial}{\partial \theta}(B_z \sin^2 \theta \cos \theta). \quad (24)$$

Noting $v = \omega r \sin \theta$, we supposed also that the magnetic field configuration depends only on the distance from the axis of rotation: $B_z = B_z(r \sin \theta) = B_z(u)$, where $u = r \sin \theta$. The reason is that, due to the Lorentz force, positive charges drift toward the external sphere and toward the equatorial plan. Using some operations (see the [appendix](#)), equation (24) is simplified and is integrated, supplying the result

$$\frac{B_2}{B_1} = \frac{\left(1 - \frac{\omega^2 R_1^2 \sin^2 \theta}{c^2}\right)}{\left(1 - \frac{\omega^2 R_2^2 \sin^2 \theta}{c^2}\right)}, \quad (25)$$

where one can see that the strengthening ratio of the magnetic field is similar to that of the cylindrical geometry, but in this case the ratio depends on the polar angle θ ; it is maximum for $\theta = \pi/2$ (in the equatorial plane), and is 1 for $\theta = 0$ (in the pole). As in the other geometries, the value of the strengthening of the magnetic field inside the laminar non relativistic fluid flows ($v \ll c$) is negligible: $B_1 \approx B_2$.

3. Discussion and conclusions

When a magnetic field is applied across the conductive fluid flows, charge carriers instantly drift until a steady redistribution of charges is settled. This instant mechanism is not a pure 'dynamo action'. We studied the spatial variation of the magnetic field in the steady state of some idealized fluid flows: laminar flow of a perfect conductive fluid. Therefore the Ohmic loss and magnetic field diffusion are not considered. The steady flows of redistributed charges produce the reconfigured magnetic field calculated here. The calculations are carried out for confined flows in different geometries: planar, cylindrical and spherical. According to our calculation of the three cases, the spatial variation of the magnetic field reconfiguration (inside the fluid) shows a strengthening i.e. the ratio of the magnetic field in two different layers: (B_2/B_1) is greater than 1 when the velocities in these layers are $v_1 < v_2$. But, this strengthening is negligible for non relativistic flows ($v_1 \ll c$ and $v_2 \ll c$). There is a slight difference between the planar geometry case and the other two cases (cylindrical and spherical geometry) regarding the ratio (B_2/B_1), which is more powerful for the last two cases. We think this difference stems from the fact that the planar geometry case enjoys infinite extension in two dimensions.

As examples, we estimated the ratio (B_2/B_1) for two real systems: the fluid flow of the Earth's outer core and the plasma of a neutron star.

If we consider the fluid flow of the Earth's outer core such as the above studied system, with $R_1 \approx 1200$ km (inner core radius), $R_2 \approx 3500$ km (outer core radius), $\omega \approx 7 \times 10^{-5} \text{ s}^{-1}$, $c = 3 \times 10^5 \text{ km s}^{-1}$, it results from equations (8) or (25)

$$B_2/B_1 \approx 1 + 6 \times 10^{-13} \approx 1.$$

The estimation of the magnetic field strengthening for rapidly spinning systems like pulsars for example, PSR J1748-244ad (Hessels *et al* 2006), where the magnetic field is very strong, the rotational period 8.8 ms and radius $R \sim 16$ km, gives $B_2/B_1 \approx 1 + 4 \cdot 10^{-2}$, where B_1 and B_2 are magnetic fields respectively for $R_1 \approx 0.3R$ and $R_2 \approx 0.9R$.

These results prove that our simple model applied to non relativistic flows, showed a negligible effect on the magnetic field reconfiguration, but the effect might not be unimportant in relativistic flows.

The configuration of the magnetic field in neutron stars is not as simple as is assumed here in the case of spherical geometry. Magnetic field decay in neutron stars is studied in detail in a substantial literature (e.g. Goldreich and Reisenegger 1992, Reissenegger 2007, Marchant *et al* 2014). Goldreich and Reisenegger (1992) studied three mechanisms that promote the losses of magnetic flux from an isolated neutron star: ohmic decay, ambipolar diffusion and Hall drift. They concluded that ohmic dissipation and ambipolar diffusion always act to decrease the magnetic energy, while in contrast Hall drift conserves magnetic energy, and it cannot be a direct cause of magnetic field decay.

Reading simplified explanations of geomagnetic field generation or stellar magnetic field generation one can have the impression that any kind of non uniform fluid flow that crosscuts a magnetic field can be a mechanism of dynamo action. However, this is an incorrect impression. Our results demonstrate that in the studied cases of non relativistic fluid flows, which are not turbulent and not convective ones, the magnetic field configuration in the steady state does not show any notable strengthening. In reality, there are complex flows of electric conductive fluids that can generate large-scale magnetic field (e.g. Kleeorin and Rogachevskii 2006, Jones 2011; etc). The magnetic fields of the planets (Fearn 1998) and Sun (Charbonneau 2014) are generated by dynamo action in their electrically conducting interiors that have usually confined spherical geometries, and the fluid flow is a convective and turbulent one (Weiss 2002). In experiments of a laboratory dynamo (cylindrical or spherical setups), there is always a differential rotation and convection of the high conductive fluid (e.g. Marie *et al* 2002, Monchaux *et al* 2007).

Even when the effect of turbulent motions is assumed to average out, for example in a trial theory of the large scale magnetic field (galactic magnetic field) origin, two ingredients need to be considered (Howard and Kulsrud 1997): the differential rotation of the interstellar medium and the motion of the field lines through the interstellar medium produced by the ambipolar diffusion of the ionized component of the plasma. A primordial magnetic field under only differential rotation could not lead to a large-scale magnetic field consistent with the observations.

The idealized flows analyzed here can be seen as additional proof that differential transport or rotational fluid flow cannot produce a notable reconfiguration of an initial magnetic field inside the fluid. On the other hand, interesting results were obtained by applying known physical principles on the idealized systems considered here.

Appendix

Detailed calculations of the strengthening ratio for the spherical geometry case

Starting with equation (22)

$$\frac{\sin \theta}{r} \frac{\partial}{\partial r} (r B_z) + \frac{1}{r} \frac{\partial}{\partial \theta} (B_z \cos \theta) = \frac{\omega^2 \sin^3 \theta}{c^2 r} \frac{\partial}{\partial r} (r^3 B_z) + \frac{\omega^2 r}{c^2} \frac{\partial}{\partial \theta} (B_z \sin^2 \theta \cos \theta), \quad (\text{A1})$$

the derivatives regarding r are moved to one side and the derivatives regarding θ are moved to other side, then we have

$$\frac{\sin \theta}{r} \frac{\partial}{\partial r}(rB_z) - \frac{\omega^2 r^2 \sin^3 \theta}{c^2 r^3} \frac{\partial}{\partial r}(r^3 B_z) = \frac{\omega^2 r}{c^2} \frac{\partial}{\partial \theta}(B_z \sin^2 \theta \cos \theta) - \frac{1}{r} \frac{\partial}{\partial \theta}(B_z \cos \theta)$$

and dividing the two sides by $\sin \theta / r$, we get

$$\frac{\partial}{\partial r}(rB_z) - \frac{\omega^2 r^2 \sin^2 \theta}{c^2 r^2} \frac{\partial}{\partial r}(r^3 B_z) = \frac{\omega^2 r^2}{c^2 \sin \theta} \frac{\partial}{\partial \theta}(B_z \sin^2 \theta \cos \theta) - \frac{1}{\sin \theta} \frac{\partial}{\partial \theta}(B_z \cos \theta)$$

or

$$\frac{\partial}{\partial r} \left(rB_z - \frac{\omega^2 r^2 \sin^2 \theta}{c^2 r^2} r^3 B_z \right) = \frac{1}{\sin \theta} \frac{\partial}{\partial \theta} \left(\frac{\omega^2 r^2 \sin^2 \theta}{c^2} B_z \cos \theta - B_z \cos \theta \right).$$

Substituting here $v = \omega r \sin \theta$, we get

$$\frac{\partial}{\partial r} \left[\left(1 - \frac{v^2}{c^2} \right) r B_z \right] = - \frac{1}{\sin \theta} \frac{\partial}{\partial \theta} \left[\left(1 - \frac{v^2}{c^2} \right) B_z \cos \theta \right]. \quad (\text{A2})$$

Using the variable $u = r \sin \theta$ and the function $B_z(u)$, we have

$$\begin{aligned} & \left(1 - \frac{v^2}{c^2} \right) r \frac{dB_z}{du} \sin \theta + B_z \frac{\partial}{\partial r} \left[\left(1 - \frac{v^2}{c^2} \right) r \right] \\ &= - \frac{1}{\sin \theta} \left\{ \left(1 - \frac{v^2}{c^2} \right) \cos \theta \frac{dB_z}{du} r \cos \theta + B_z \frac{\partial}{\partial \theta} \left[\left(1 - \frac{v^2}{c^2} \right) \cos \theta \right] \right\}. \end{aligned} \quad (\text{A3})$$

The derivative in the second term of the left-hand side of equation (A3) can be calculated as follows

$$\frac{\partial}{\partial r} \left[\left(1 - \frac{v^2}{c^2} \right) r \right] = 1 - \frac{3v^2}{c^2}. \quad (\text{A4})$$

The derivative in the second term of the right-hand side of equation (A3) can be calculated as follows

$$\frac{\partial}{\partial \theta} \left[\left(1 - \frac{v^2}{c^2} \right) \cos \theta \right] = - \sin \theta \left(1 - \frac{3v^2}{c^2} \right) - \frac{1}{\sin \theta} \frac{2v^2}{c^2}. \quad (\text{A5})$$

Substituting (A4) and (A5) in (A3), and rearranging terms, we have

$$\left(1 - \frac{v^2}{c^2} \right) \left[r \sin \theta + \frac{r \cos^2 \theta}{\sin \theta} \right] \frac{dB_z}{du} = -B_z \left[1 - \frac{3v^2}{c^2} - 1 + \frac{3v^2}{c^2} - \frac{1}{\sin^2 \theta} \cdot \frac{2v^2}{c^2} \right]$$

or

$$\left(1 - \frac{v^2}{c^2} \right) \cdot \frac{r \sin \theta}{\sin^2 \theta} \frac{dB_z}{du} = B_z \cdot \frac{1}{\sin^2 \theta} \frac{2v^2}{c^2}. \quad (\text{A6})$$

Manipulating (A6), we get

$$\frac{dB_z}{B_z} = \frac{2\omega^2 u^2}{c^2 \left(1 - \frac{\omega^2 u^2}{c^2} \right)} \frac{du}{u} = - \frac{d \left(- \frac{\omega^2 u^2}{c^2} \right)}{\left(1 - \frac{\omega^2 u^2}{c^2} \right)} \implies \frac{dB_z}{B_z} = - \frac{d \left(1 - \frac{\omega^2 u^2}{c^2} \right)}{\left(1 - \frac{\omega^2 u^2}{c^2} \right)}, \quad (\text{A7})$$

Integrating (A7)

$$\ln(B_z)_{B_1}^{B_2} = -\ln\left(1 - \frac{\omega^2 u^2}{c^2}\right)_{B_1}^{B_2} \implies \frac{B_2}{B_1} = \frac{\left(1 - \frac{\omega^2 R_1^2 \sin^2 \theta}{c^2}\right)}{\left(1 - \frac{\omega^2 R_2^2 \sin^2 \theta}{c^2}\right)} \quad (\text{A8})$$

$$\text{For } \theta = 0, B_2/B_1 = 1 \text{ and for } \theta = \pi/2 \frac{B_2}{B_1} = \frac{\left(1 - \frac{\omega^2 R_1^2}{c^2}\right)}{\left(1 - \frac{\omega^2 R_2^2}{c^2}\right)}.$$

References

- Charbonneau P 2014 Solar dynamo theory *Annu. Rev. Astron. Astrophys.* **52** 251–90
- Cooper C M *et al* 2014 The Madison plasma dynamo experiment: a facility for studying laboratory plasma astrophysics *Phys. Plasmas* **21** 013505
- Duka B 1999 Could be the rotation of Earth's inner core as the cause of dipolar magnetic field generation? *Il Nuovo Cimento* **22** 191–206
- Fearn D R 1998 Hydromagnetic flow in planetary cores *Rep. Prog. Phys.* **61** 175–235
- Gailitis A, Lielausis O, Platacis E, Dement'ev S, Cifersons A, Gerbeth D, Gundrum T, Stefani F, Christen M and Will G 2002 Dynamo experiments at the Riga sodium facility *Special Issue of Magneto-Hydrodynamics* **38** 5–14
- Giesecke A, Nore C, Stefani F, Gerbeth G, Léorat J, Herreman W, Luddens F and Guermond J L 2012 Influence of high-permeability discs in an axisymmetric model of the Cadarache dynamo experiment *New J. Phys.* **14** 053005
- Goldreich P and Reisenegger A 1992 Magnetic field decay in isolated neutron stars *Astrophys. J.* **395** 250–8
- Hessels J W T, Ransom S M, Stairs I H, Freire P C C, Kaspi V M and Camilo F 2006 A radio pulsar spinning at 716 Hz *Science* **311** 1901–4
- Howard A M and Kulsrud R M 1997 The evolution of a primordial galactic magnetic field *Astrophys. J.* **483** 648–65
- Inglis D R 1981 Dynamo theory of the Earth's varying magnetic field *Rev. Mod. Phys.* **53** 481
- Jackson D 1999 *Classical Electrodynamics* (New York: Wiley)
- Jones C A 2011 Planetary magnetic fields and fluid dynamos *Annu. Rev. Fluid Mech.* **43** 583–614
- Kleeorin N and Rogachevskii I 2006 Effect of heat flux on differential rotation in turbulent convection *Phys. Rev. E* **73** 046303
- Kuang W and Bloxham J 1997 An Earth-like numerical dynamo model *Nature* **389** 371–4
- Kunkel W B 1981 Hall effect in plasma *Am. J. Phys.* **49** 733–8
- Landau L D and Lifshitz E M 1987 *Fluid mechanics Theoretical Physics* vol 6 2nd edn (Oxford: Pergamon)
- Love A 1999 Reversals and excursions of the geodynamo *Astron. Geophys.* **40** 14–19
- Lowes F J and Wilkinson I 1963 Geomagnetic dynamo: a laboratory model *Nature* **198** 1158
- Marchant P, Reisenegger A, Valdivia J A and Hoyos J H 2014 Stability of Hall equilibria in neutron star crusts *Astrophys. J.* **796** 94
- Marie L, Petrelis F, Bourgoin M, Burguete J, Chiffaudel A, Daviaud F, Fauve S, Odier P and Pintonet J-F 2002 Open questions about homogeneous fluid dynamos: the VKS experiment *Special Issue of Magneto-Hydrodynamics* **38** 163–76
- Moelter M J, Evans J, Elliott G and Jackson M 1998 Electric potential in the classical Hall effect: an unusual boundary-value problem *Am. J. Phys.* **66** 668
- Moffatt H K 1978 *Magnetic Field Generation in Electrically Conducting Fluids* (Cambridge: Cambridge University Press)
- Monchaux R *et al* 2007 Generation of a magnetic field by dynamo action in a turbulent flow of liquid sodium *Phys. Rev. Lett.* **98** 044502

- Müller U and Stieglitz R 2002 The karlsruhe dynamo experiment *Nonlinear Process. Geophys.* **9** 165–70
- Ogilvie G I 2016 Astrophysical fluid dynamics *J. Plasma Phys.* **82** 205820301
- Parker E 1979 *Cosmical Magnetic Fields* (New York: Oxford University Press)
- Petersen D H, Hansen O, Lin R and Nielsen P F 2008 Micro-four-point probe Hall effect measurement method *J. Appl. Phys.* **104** 13710
- Reissenegger A 2007 Magnetic field evolution in neutron stars *Astron. Nachr.* **328** 997–1177
- Roberts P H and Glatzmaier G A 2000 Geodynamo theory and simulations *Rev. Mod. Phys.* **72** 1081
- Roberts P H and Soward A M 1992 Dynamo theory *Ann. Rev. Fluid Mech.* **24** 459–512
- Sarson G R and Jones C A 1999 A convection driven geodynamo reversal model *Phys. Earth Planet. Inter.* **111** 3–20
- Spence E, Reuter K and Forest C B 2009 Numerical simulations of a spherical plasma dynamo experiment *Astrophys. J.* **700** 470
- Stieglitz R and Muller U 2001 Experimental demonstration of a homogeneous two-scale dynamo *Phys. Fluids* **13** 561
- Stix M 2002 *The Sun: An Introduction* (Berlin: Springer)
- Turkyilmazoglu M 2012 Exact solutions for the incompressible viscous magnetohydrodynamic fluid of a porous rotating disk flow with Hall current *Int. J. Mech. Sci.* **56** 86–95
- Turkyilmazoglu M 2010 Heat and mass transfer on the MHD fluid flow due to a porous rotating disk with hall current and variable properties *J. Heat Transfer* **133** 021701
- Weiss N 2002 Dynamos in planets, stars, and galaxies *Astron. Geophys.* **43** 9–14